

Nonlocal composite media in calculations of the Casimir force

J. Sun,^{1,2,*} Y. Huang,^{1,*†} and L. Gao^{1,‡}

¹*Jiangsu Key Laboratory of Thin Films, Department of Physics, Soochow University, Suzhou 215006, China*

²*Department of Mathematics and Physics, Suzhou University of Science and Technology, Suzhou 215009, China*

(Received 24 August 2013; published 16 January 2014)

The Casimir force between two inhomogeneous metal-dielectric composite slabs with spatial dispersion is investigated theoretically. The equivalent permittivity and permeability of the nonlocal metallic nanosphere is originally derived based on full-wave nonlocal Mie theory. We then adopt two nonlocal effective medium models to study the effective permittivity and permeability of the composite slabs and calculate the Casimir force with Casimir-Lifshitz theory. Due to the excitation of the longitudinal modes, the attractive Casimir force between nonlocal composite materials is much weaker than that of the local composites, and numerical results show that the relative errors between local and nonlocal calculations of Casimir force can be on the order of 25%. Moreover, the nonlocal effects on the Casimir force are strongly dependent on the microstructures, and they become significant near the percolation threshold of the composite media. The study may be of great interest for making a precise comparison between theoretical and experimental results on the Casimir force between inhomogeneous composite materials.

DOI: [10.1103/PhysRevA.89.012508](https://doi.org/10.1103/PhysRevA.89.012508)

PACS number(s): 31.30.jh, 03.65.Ud, 77.84.Lf, 78.67.Bf

I. INTRODUCTION

The Casimir force [1] results from the spatial redistribution of the fluctuations of the electromagnetic field in comparison with that of free space because of the presence of two parallel uncharged conductors. Actually, it demonstrates the reality of zero-point field fluctuations. During past decades, the Casimir force received much attention due to its potential applications in nanoscience [2,3] such as in micro- and nanoelectromechanical systems (MNEMS).

Recently, the Casimir force between two parallel slabs containing homogeneous electromagnetic materials was investigated with the Casimir-Lifshitz theory [4–7]. The behavior of the Casimir force is found to be largely dependent on the permittivity and permeability of the electromagnetic materials [8–10]. With the development of artificial metamaterials, it is expected to obtain the repulsive and restoring Casimir force between two metamaterials' slabs [11–13]. In addition, the Casimir force between inhomogeneous materials provides additional issues in the evaluation of the Casimir force. For instance, the magnitude of the Casimir force in aerogels (the two-phase composite materials in which air bubbles are embedded in the SiO₂ host medium) was reduced [14]. Physical restrictions on the Casimir interaction of metal-dielectric metamaterials with the aid of the effective medium theory were investigated [15]. Later, a multilayered effective medium model was proposed to evaluate the contribution of surface roughness to the Casimir force [16]. Much effort was devoted to the discussion on the divergence of Casimir force within the Casimir theory for the case of inhomogeneous media [17–20]. Esquivel-Sirvent *et al.* found that the use of composite materials to modify the Casimir force required careful investigation of the effective electromagnetic properties of the composites, and the magnitude of the force was very sensitive

to the choices of effective medium theories [21]. We predicted that it is possible to enhance the Casimir force by taking into account the particles' shape in inhomogeneous composite media [22].

On the other hand, with the significant development of science and technology, the size scale of composite materials or films can be down to a few nanometers (about 10 nm). In this regard, the nonlocal effect should be taken into account. The nonlocality or spatial dispersion means that the permittivity (or the permeability) of the material is dependent not only on the incident frequency ω , but also on the wave vector \mathbf{k} . Some scientists investigated the spatial dispersion or nonlocal effect in the study of the Casimir force between two homogeneous slabs [23–27]. For the homogeneous slabs, a surface impedance approach including the nonlocality was introduced to study the reflection coefficients and, hence, the Casimir force. Numerical results show that the difference between local and nonlocal calculations of the Casimir force is of the order of a few tenths of a percent [26,27]. Incidentally, the Casimir interaction and the Hamaker coefficients between two Au nanospheres or nanorods with spatial dispersion were calculated [28]. Due to the interaction between the nonlocality and the inhomogeneity, one expects that the nonlocal effects on the Casimir force between inhomogeneous slabs may become strong. However, the spatial dispersion on the Casimir force between inhomogeneous composite materials has not been considered [21,22].

In this paper, we study the Casimir force between inhomogeneous composite materials by taking into account the spatial dispersion or nonlocal effect. The composite systems consist of nonlocal metallic nanospheres with volume fraction f , and dielectric particles with volume fraction $1 - f$. In order to take into account the spatial dispersion, we derive the equivalent permittivity ϵ_{equiv} and permeability μ_{equiv} of the metallic nanosphere with spatially dispersive permittivity $\epsilon(\omega, \mathbf{k})$ by considering the scattering problem [29] of the nonlocal metallic sphere in an equivalent medium [30]. Then, we adopt two common effective medium theories, the Bruggeman effective medium theory and Maxwell-Garnett theory, to

*These authors contributed equally to this work.

†yanghuang808@163.com

‡leigao@suda.edu.cn

estimate the effective permittivity ε_e and permeability μ_e of the inhomogeneous composite materials. One can take one step forward to investigate the nonlocal effect on the Casimir force between two inhomogeneous composite materials with the aid of Casimir-Lifshitz theory.

The paper is organized as follows. In Sec. II, we first outline the Casimir-Lifshitz theory for the Casimir force between two infinite slabs made of metal-dielectric nanocomposite materials with spatial dispersion, and Bruggeman effective medium theory and Maxwell-Garnett theory are briefly introduced to investigate the effective magnetoelectric properties of the infinite composites slabs. In particular, we establish the equivalent theory for the equivalent local permittivity and permeability of the nonlocal metallic nanosphere. In Sec. III, numerical results about nonlocal effects on the Casimir forces are shown. Our conclusions and discussion are presented in Sec. IV.

II. MODEL AND THEORY

Let us consider the Casimir force between two semi-infinite composite slabs separated by a distance d with Casimir-Lifshitz theory. Each composite slab is composed of the spherical metallic particles with nonlocal permittivity $\varepsilon(\omega, k)$ and the volume fraction f , and the dielectric component with local permittivity ε_2 and the volume fractions $1 - f$. Without loss of generality, both metal and dielectric components are assumed to be nonmagnetic with $\mu_i = 1$ ($i = 1, 2$). The Casimir-Lifshitz theory for the Casimir force is valid for the given temperature, which includes the term for the zero-point fluctuations (or the term at zero temperature) and the finite-temperature (or thermal-force) term [4,6]. Generally, when the separation distance between two slabs d (in our calculations, $d \sim 100\text{--}500$ nm) is much smaller than a typical length $\hbar c/k_B T$ ($\hbar c/k_B T \sim 7 \mu\text{m}$ for $T = 300$ K), the temperature corrections can usually be negligible [31,32]. In addition, we aim at the effect of spatial dispersion on the Casimir force. In what follows, we concentrate on the Casimir force at zero temperature only.

A. The Casimir force at zero temperature

Based on the stress tensor method, the Casimir force per unit area at zero temperature between two parallel, infinite slabs can be written as [5–7]

$$F_C(d) = \frac{\hbar}{2\pi^2} \int_0^\infty d\xi \int_0^\infty k dk \sqrt{\frac{\xi^2}{c^2} + k^2} \times \sum_{N=\text{TE, TM}} \frac{r_N^2(\xi, k) e^{-2d\sqrt{\frac{\xi^2}{c^2} + k^2}}}{1 - r_N^2(\xi, k) e^{-2d\sqrt{\frac{\xi^2}{c^2} + k^2}}}, \quad (1)$$

where k is the transverse wave vector parallel to the slab surface, and r_N is the reflection coefficient of each slab for the transverse electric ($N = \text{TE}$) and transverse magnetic ($N = \text{TM}$) polarization waves. For simplicity, we have introduced the imaginary frequency ξ with $\omega = i\xi$. In addition, the reflection coefficients for the infinite slab in Eq. (1) are

expressed as

$$r_{\text{TE}} = \frac{\mu_e(i\xi)\sqrt{k^2 + \xi^2/c^2} - \sqrt{k^2 + \varepsilon_e(i\xi)\mu_e(i\xi)\xi^2/c^2}}{\mu_e(i\xi)\sqrt{k^2 + \xi^2/c^2} + \sqrt{k^2 + \varepsilon_e(i\xi)\mu_e(i\xi)\xi^2/c^2}}, \quad (2)$$

$$r_{\text{TM}} = \frac{\varepsilon_e(i\xi)\sqrt{k^2 + \xi^2/c^2} - \sqrt{k^2 + \varepsilon_e(i\xi)\mu_e(i\xi)\xi^2/c^2}}{\varepsilon_e(i\xi)\sqrt{k^2 + \xi^2/c^2} + \sqrt{k^2 + \varepsilon_e(i\xi)\mu_e(i\xi)\xi^2/c^2}}, \quad (3)$$

where ε_e and μ_e are, respectively, the permittivity and permeability of the infinite slab. In our situation, since the infinite slab is not a homogenous material but an inhomogeneous composite one, ε_e and μ_e should be the effective permittivity and permeability of the composite system at the imaginary frequency. After performing the polar coordinates transformation $\xi/c = x \cos \phi$, $k = x \sin \phi$, we obtain the normalized force $\eta(d)$, defined as the ratio of the force to the Casimir force between two perfectly conducting plates F_0 ($= \pi^2 \hbar c / 240 d^4$) [5],

$$\eta(d) = \frac{120d^4}{\pi^4} \int_0^\infty dx x^3 \int_0^{\pi/2} \sin \phi d\phi \times \sum_{N=\text{TE, TM}} \frac{r_N^2(x, \phi) e^{-2dx}}{1 - r_N^2(x, \phi) e^{-2dx}}. \quad (4)$$

B. Effective medium theories

To calculate the effective permittivity and permeability of composite slabs including the spatial dispersion, we adopt two popular effective medium models: one is for the symmetrical microgeometry, in which both the spherical metallic nanoparticles and dielectric nanoparticles are randomly distributed, and the other describes the asymmetrical microgeometry, in which the nanometallic particles are randomly embedded in the dielectric host. For the former, the effective permittivity and permeability of the composite system are given by Bruggeman effective medium theory,

$$f \left(\frac{\varepsilon_{\text{equiv}} - \varepsilon_e}{\varepsilon_{\text{equiv}} + 2\varepsilon_e} \right) + (1 - f) \left(\frac{\varepsilon_2 - \varepsilon_e}{\varepsilon_2 + 2\varepsilon_e} \right) = 0 \quad \text{and} \quad (5)$$

$$f \left(\frac{\mu_{\text{equiv}} - \mu_e}{\mu_{\text{equiv}} + 2\mu_e} \right) + (1 - f) \left(\frac{1 - \mu_e}{1 + 2\mu_e} \right) = 0,$$

where $\varepsilon_{\text{equiv}}$ and μ_{equiv} are the equivalent permittivity and permeability of the nonlocal metallic particles and are derived in the next sections.

For the latter model, the effective permittivity and permeability of the composite system can be described within Maxwell-Garnett theory,

$$\frac{\varepsilon_e - \varepsilon_2}{\varepsilon_e + 2\varepsilon_2} = f \frac{\varepsilon_{\text{equiv}} - \varepsilon_2}{\varepsilon_{\text{equiv}} + 2\varepsilon_2} \quad \text{and} \quad \frac{\mu_e - 1}{\mu_e + 2} = f \frac{\mu_{\text{equiv}} - 1}{\mu_{\text{equiv}} + 2}. \quad (6)$$

C. Equivalent physical parameters for nonlocal metal nanoparticles

We are now in a position to investigate the equivalent permittivity $\varepsilon_{\text{equiv}}$ and equivalent permeability μ_{equiv} for the nonlocal metallic nanoparticles. For this purpose, we consider the scattering problem of a nonlocal metallic nanosphere with

nonlocal permittivity $\varepsilon(\omega, k)$ and the radius a in an effective medium with the permittivity $\varepsilon_{\text{equiv}}$ and permeability μ_{equiv} [30,33].

For the nonlocal sphere, we assume the hydrodynamic model to describe its longitudinal permittivity [24,34],

$$\varepsilon_L(\omega, k) = \varepsilon_g - \frac{\omega_p^2}{\omega^2 + i\omega\gamma - \beta^2 k^2}, \quad (7)$$

where ε_g is the background permittivity of the metals due to interband transitions, ω_p is the plasma frequency, γ is the damping constant, and $\beta = \sqrt{3/5}v_F$ with v_F being the Fermi velocity of electrons in a metal. In addition, we have the transverse permittivity $\varepsilon_T(\omega) = \varepsilon(\omega, 0)$. Both longitudinal and

transverse waves can be propagated in the nonlocal system, and the wave vector of a longitudinal electromagnetic wave k_L propagating in the nonlocal nanosphere is determined by the equation $k_L(\omega) = \sqrt{(\omega^2 + i\omega\gamma - \omega_p^2/\varepsilon_g)/\beta^2}$, while the transverse electromagnetic mode satisfies the dispersion relation $k_T^2(\omega) = \omega^2/c^2\varepsilon_T(\omega)$ [29]. For the local case, β should be zero and Eq. (7) is nothing but the Drude permittivity for the metal.

For the plane electromagnetic wave, after neglecting the common parts of the fields $E_0 e^{-i\omega t} \sum_{l=1}^{\infty} i^l \frac{2l+1}{l(l+1)}$, the incident \mathbf{E}_I and scattering \mathbf{E}_R electric fields, the transverse \mathbf{E}_T and the longitudinal \mathbf{E}_L electric fields inside the nanoparticle can be written as [29,35,36]

$$\begin{aligned} \mathbf{E}_I &= \nabla \times [\mathbf{r} j_l(k_{\text{equiv}} r) P_l^{(1)}(\cos \theta) \sin \phi] - \frac{i}{k_{\text{equiv}}} \nabla \times \nabla \times [\mathbf{r} j_l(k_{\text{equiv}} r) P_l^{(1)}(\cos \theta) \cos \phi], \\ \mathbf{E}_R &= a_l^R \nabla \times [\mathbf{r} h_l(k_{\text{equiv}} r) P_l^{(1)}(\cos \theta) \sin \phi] - b_l^R \frac{i}{k_{\text{equiv}}} \nabla \times \nabla \times [\mathbf{r} h_l(k_{\text{equiv}} r) P_l^{(1)}(\cos \theta) \cos \phi], \\ \mathbf{E}_T &= a_l^T \nabla \times [\mathbf{r} j_l(k_T r) P_l^{(1)}(\cos \theta) \sin \phi] - b_l^T \frac{i}{k_T} \nabla \times \nabla \times [\mathbf{r} j_l(k_T r) P_l^{(1)}(\cos \theta) \cos \phi], \\ \mathbf{E}_L &= \frac{b_l^L}{k_L} \nabla [j_l(k_L r) P_l^{(1)}(\cos \theta) \cos \phi], \end{aligned} \quad (8)$$

where $j_l(\dots)$ [or $h_l(\dots)$] represents spherical Bessel (or Hankel) functions, and $k_{\text{equiv}} = \omega \sqrt{\varepsilon_{\text{equiv}} \mu_{\text{equiv}}} / c$. Moreover, the corresponding magnetic fields can be obtained from the Maxwell equation $\mathbf{H} = (\nabla \times \mathbf{E}) / i\omega\mu$. Note that there is no corresponding longitudinal magnetic field inside the nonlocal sphere.

In above equations, five unknown coefficients a_l^R , b_l^R , a_l^T , b_l^T , and b_l^L should be determined by the boundary conditions on the spherical surface. In general, the continuity conditions of the tangential components of the electric and magnetic fields would be matched on the interface between the metallic nanosphere and the outer effective medium at $r = a$. In addition, due to the excitation of the longitudinal mode inside the nonlocal sphere, an additional boundary condition should be required [37,38]. Here, without loss of generality, we adopt the additional boundary condition in Ref. [38]. After some tedious calculations, the solutions for the coefficients a_l^R and b_l^R of the scattered wave are

$$a_l^R = -\frac{j_l(k_T a)[k_{\text{equiv}} a j_l(k_{\text{equiv}} a)]' - \mu_{\text{equiv}} j_l(k_{\text{equiv}} a)[k_T a j_l(k_T a)]'}{j_l(k_T a)[k_{\text{equiv}} a h_l(k_{\text{equiv}} a)]' - \mu_{\text{equiv}} h_l(k_{\text{equiv}} a)[k_T a j_l(k_T a)]'} \quad (9)$$

$$b_l^R = -\frac{\varepsilon_T j_l(k_T a)[k_{\text{equiv}} a j_l(k_{\text{equiv}} a)]' - \varepsilon_{\text{equiv}} j_l(k_{\text{equiv}} a)[k_T a j_l(k_T a)]' + Q_l j_l(k_{\text{equiv}} a)}{\varepsilon_T j_l(k_T a)[k_{\text{equiv}} a h_l(k_{\text{equiv}} a)]' - \varepsilon_{\text{equiv}} h_l(k_{\text{equiv}} a)[k_T a j_l(k_T a)]' + Q_l h_l(k_{\text{equiv}} a)} \quad (10)$$

with $Q_l = \varepsilon_{\text{equiv}} l(l+1)(\varepsilon_g - \varepsilon_T) j_l(k_T a) j_l(k_L a) / [\varepsilon_g k_L a j_l'(k_L a)]$.

The total scattering cross section is written as $\sigma_{\text{sca}} = 2\pi/k_{\text{equiv}}^2 \sum_{l=1}^{\infty} (2l+1)(|a_l^R|^2 + |b_l^R|^2)$. In the case of $k_{\text{equiv}} a \ll 1$, σ_{sca} is dominated by the dipole terms a_1^R and b_1^R . For a scattering nonlocal particle inside a homogenous background medium with constitutive parameters $\varepsilon_{\text{equiv}}$ and μ_{equiv} , if σ_{sca} tends to be zero (or a_1 and b_1 are zero), the electromagnetic field outside the nonlocal sphere will be undisturbed. Then one can judge that $\varepsilon_{\text{equiv}}$ and μ_{equiv} are the equivalent constitutive parameters for the nonlocal particle. Therefore, we can set the conditions for the equivalent medium as $a_1^R = 0$ and $b_1^R = 0$ [30,39] and obtain

$$\varepsilon_{\text{equiv}} = \frac{2\varepsilon_g j_1(k_T a) j_1'(k_L a)}{\varepsilon_g [k_T a j_1(k_T a)]' j_1'(k_L a) - 2(\varepsilon_g - \varepsilon_T) j_1(k_T a) j_1(k_L a) / (k_L a)} \varepsilon_T, \quad (11)$$

$$\mu_{\text{equiv}} = \frac{2j_1(k_T a)}{[k_T a j_1(k_T a)]'}. \quad (12)$$

In deriving the above equations, we approximate the functions $j_1(x) \cong x/3$ and $h_1(x) \cong x/3 - i/x^2$ as $x \ll 1$. Equations (11) and (12) are our original formulas for the equivalent permittivity and permeability of the nonlocal metallic sphere

with spatial dispersion. The equivalent theory is derived based on the generalized Mie theory of nonlocal spheres and, hence, is beyond the electrostatic approximation. If one neglects the spatial dispersion of the metal, the nanosphere cannot support

longitudinal polarization waves and the imaginary part of k_L becomes infinitely large [29]. Substituting $\text{Im}(k_L) \rightarrow \infty$ into Eqs. (11) and (12) results in

$$\varepsilon_{\text{equiv}} = \varepsilon_T \frac{2j_1(k_T a)}{[k_T a j_1(k_T a)]'} \quad \text{and} \quad \mu_{\text{equiv}} = \frac{2j_1(k_T a)}{[k_T a j_1(k_T a)]'}, \quad (13)$$

which are just the same as those within local descriptions [30,40]. Furthermore, if we consider the electrostatic limit $k_T a \ll 1$, $\varepsilon_{\text{equiv}}$ and μ_{equiv} will, respectively, tend to be ε_T and 1, as expected. Equations (11) and (12) indicate that equivalent physical parameters are dependent on the radius of the nonlocal nanosphere. This is quite similar to the case of differential effective medium theory developed for the graded particles, in which the local permittivity varies continuously in space [41,42].

According to our theory, the electromagnetic properties of metal particles with spatial dispersion can be well described by the equivalent physical parameters $\varepsilon_{\text{equiv}}$ and μ_{equiv} . For the calculation of the Casimir force between the composite slabs containing nonlocal metal nanoparticles, the equivalent permittivity $\varepsilon_{\text{equiv}}$ and permeability μ_{equiv} should be calculated from the real-imaginary frequency transformation $\omega = i\xi$ with Eqs. (11) and (12). Then the effective permittivity ε_e and permeability μ_e of the composite slab are evaluated with Eqs. (5) and (6). For brevity, we name them nonlocal effective medium theory (NEMT) and nonlocal Maxwell-Garnett theory (NMGT), in contrast to local effective medium theory (EMT) and Maxwell-Garnett theory (MGT), respectively. For EMT and MGT, we still are beyond the electrostatic approximation and substitute Eq. (13) into Eqs. (5) and (6). We should remark that an alternative nonlocal effective medium theory for the symmetric composite system can be derived based on the self-consistent approach [43], and it might be a better treatment to model the effective constitutive parameters of the composite slab with symmetric microstructures. However, it is found to give almost the same results as our NEMT (not shown here). Then the Casimir force between the composite slabs including the nonlocal effect can be determined with Casimir-Lifshitz theory. The substitution of the equivalent physical parameters of nonlocal nanosphere into the effective medium theories was adopted in a similar way in Ref. [44] to investigate the Goos-Hanchen shift at an interface of composite materials containing nonlocal metallic nanoparticles.

III. NUMERICAL RESULTS

In what follows, we calculate the Casimir force between two infinite Au-SiO₂ composite slabs containing metal nanoparticles with spatial dispersion. For this purpose, the relevant parameters for Au with spatial dispersion are the plasma frequency $\omega_p = 9.0$ eV, the damping coefficient $\gamma = 0.035$ eV, and the Fermi velocity $v_F = 1.36 \times 10^6$ m/s [37]; the permittivity of SiO₂ in the imaginary frequency is given in Ref. [21].

In Fig. 1, the effective permittivity ε_e and permeability μ_e of the inhomogeneous composite materials containing nonlocal spheres with symmetric microstructures [Eq. (5)] and asymmetric microstructures [Eq. (6)] are plotted as a

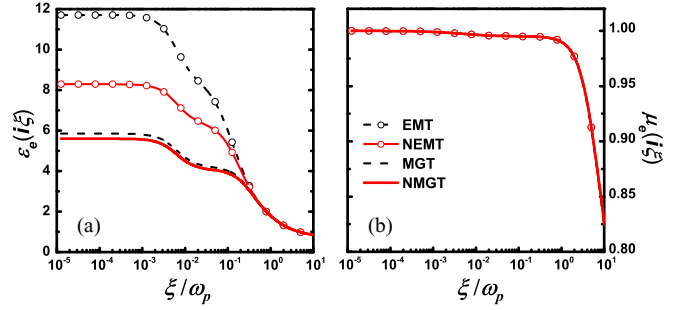


FIG. 1. (Color online) (a) The effective permittivity ε_e and (b) the permeability μ_e plotted as a function of the normalized imaginary frequency ξ/ω_p for $a = 10$ nm and $f = 0.25$.

function of the normalized imaginary frequency ξ/ω_p . The results for local cases are also shown for comparison. At first, we aim at the effective permittivity [see Fig. 1(a)]. It is seen that the permittivity of Au is quite large for low frequencies from the Drude form for the permittivity. Physically, the large permittivity results from the pole at zero frequency in the Drude permittivity, which is responsible for the dc conductivity [21]. Therefore, in the low-frequency region, the permittivity of Au will dominate the behavior of the composites, resulting in large effective permittivity. Furthermore, the Bruggeman effective medium theory predicts much larger effective permittivity than Maxwell-Garnett theory. On the contrary, for high frequencies, the permittivity of Au decreases and is comparable to that of dielectric components. As a consequence, one observes small effective permittivity and both theories give very similar results. Second, when the nonlocality is taken into account, one finds that the effective permittivities with nonlocal theories are smaller than that with local theories, and the difference becomes significant for the composite materials with symmetric microstructure especially in the low-frequency region [see Fig. 1(a)]. As far as the effective permeability is concerned [see Fig. 1(b)], because our method is beyond the electrostatic approximation, the equivalent permeability will not be 1 for both local and nonlocal theories. This indicates that the composite material will exhibit magnetic properties, characterized by $\mu_e \neq 1$, although its components are nonmagnetic with $\mu = 1$.

To understand the dependence of the Casimir force on the spatial dispersion, we study the behavior of the reflection coefficients for TE and TM polarization waves in Fig. 2. Here, the characteristic wave number k is taken to be 5×10^5 for illustration [26]. For both TE and TM polarization waves, it is evident that the magnitude of the reflection coefficient $|r_{\text{TE}}|$ for NEMT is less than that for EMT, whereas NMGT and MGT give very similar results. Qualitatively, when the nonlocality is included, it needs additional electromagnetic energies to excite the confined longitudinal modes, in addition to exciting the transverse electromagnetic modes. As a consequence, one expects small refractivity for the composite materials containing nonlocal metallic nanoparticles. Note that, above the frequency $\xi = 10\omega_p$, both r_{TE} and r_{TM} are close to zero and, hence, few virtual photons exist in the cavity between two inhomogeneous composite materials. Therefore, to perform the integral for the calculations of the Casimir force, one

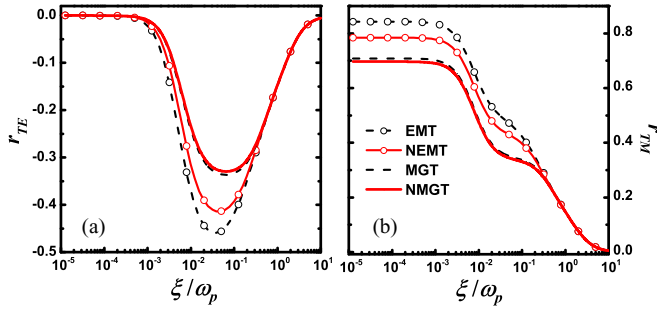


FIG. 2. (Color online) The reflection coefficients (a) r_{TE} and (b) r_{TM} of the composite material plotted as a function of the imaginary frequency ξ for $k = 5 \times 10^5$. Other parameters are the same as those in Fig. 1.

adopts the cutoff frequency, above which there is almost no contribution to the Casimir force [10,21].

Next, we aim at the effect of the volume fraction f on the normalized Casimir force η between two inhomogeneous composite slabs with spatial dispersion in Fig. 3. For comparison, the results for EMT and MGT are also shown. The value of η is increased monotonically as the volume fraction increases for all the cases, which is quite similar to those reported for the local composite systems [21,22]. For the asymmetrical microstructures, it is shown that the Casimir force with NMGT is practically identical to that with MGT, and the difference between two cases is quite small. However, for the symmetrical microstructures, the nonlocality plays an important role in the Casimir force, and the difference between NEMT and EMT is quite large, especially for large volume fractions. We understand this as follows: for the symmetrical microstructures, both NEMT and EMT predict the percolation threshold at $f_c = 1/3$, above which the metal nanoparticles easily form infinite connected clusters throughout the whole composite, resulting in the metallic property of the composite slab [22,40]. In this connection, the nonlocal effect becomes very important. However, for asymmetrical microstructures, the metal nanoparticles are always surrounded by the dielectric host medium and no percolation takes place. Thus, the

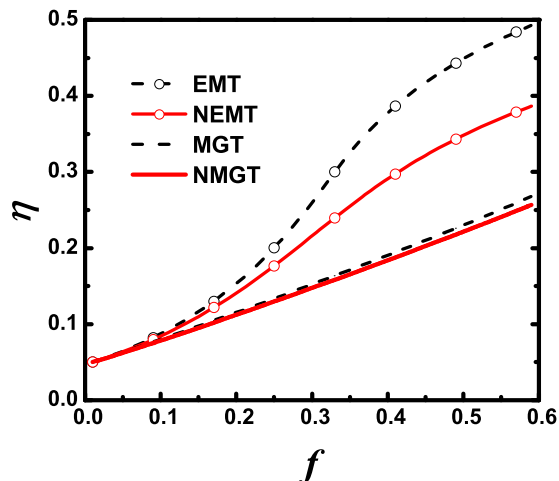


FIG. 3. (Color online) η vs f for $d = 200$ nm.

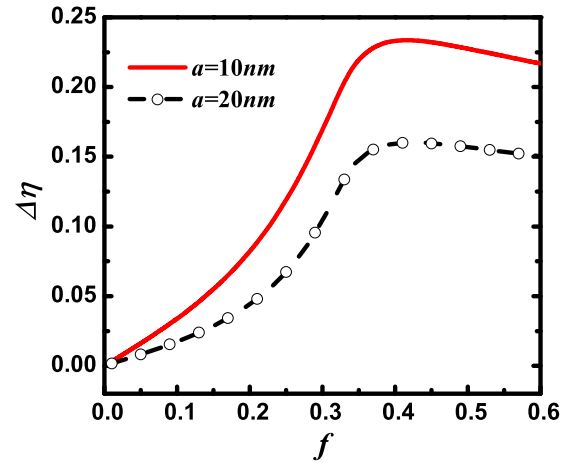


FIG. 4. (Color online) $\Delta\eta$ as a function of f for symmetrical microstructures for $d = 200$ nm.

nonlocality on the Casimir force is relatively weak. Therefore, we conclude that, for inhomogeneous composite slabs, the nonlocal effects on the Casimir force are sensitively dependent on the microgeometrical structures of the composite media, and the suitable choice of the effective medium approximations is very important to predict the Casimir force accurately.

Here, we would like to add some possible explanations on the point that the introduction of spatial dispersion leads to the decrease of the Casimir force. As shown in Fig. 2, the reflections of electromagnetic radiation at the interface between the composite slabs and vacuum for the nonlocal case are fewer than those for the local case; hence, the density of electromagnetic energy confined in the vacuum cavity will be diminished. As a consequence, we predict small Casimir force between the composite slabs containing nonlocal metallic nanoparticles in comparison with that for the local case. In order to quantify nonlocal effects on the Casimir force between the composite materials with symmetrical microstructures, we calculate the relative error between the local Casimir force η_{EMT} and the nonlocal one η_{NEMT} by using $\Delta\eta = |\eta_{NEMT} - \eta_{EMT}|/\eta_{EMT}$ in Fig. 4. It is evident that, for given sizes $a = 10$ and 20 nm, there is a critical volume fraction near which the relative error $\Delta\eta$ is maximal. Actually, this critical volume fraction is just the percolation threshold $f_c = 1/3$, independent of the size of metallic nanoparticles. Therefore, the relative error achieves the maximum and the nonlocal effect is strongest at the percolation threshold. Note that the relative error between the local and the nonlocal cases can be of the order of 25% at f_c , in contrast to a quite small difference between nonlocal and local calculations on the Casimir force between homogeneous slabs [27]. In addition, the relative error increases with decreasing the radius a , and the nonlocal effect on the Casimir force becomes more and more important for small size a , as expected.

In the end, we plot the normalized Casimir force between the composite slabs with symmetric microstructures and the relative error as a function of the distance d in Fig. 5. Both EMT and NEMT predict that the Casimir force exhibits monotonic increase with increasing d [see Fig. 5(a)]. Actually, it is known that the main contribution to the Casimir force results from

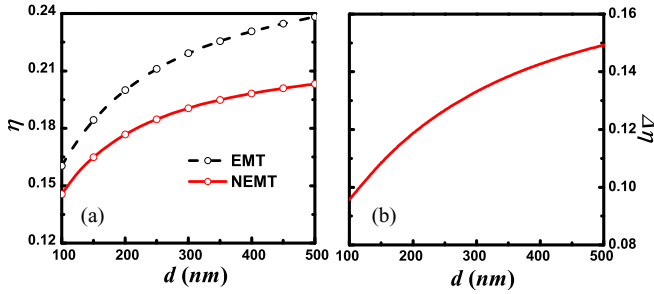


FIG. 5. (Color online) η and $\Delta\eta$ vs d for symmetrical microstructures for $a = 10$ nm.

the frequencies $\xi < c/d$ [45,46]. For small (or large) d , the weight of the contribution from the high-frequency (or low-frequency) region in the Casimir force will increase. Since the effective permittivity of the composite slabs in the high-frequency (or low-frequency) region is small (or large), one observes small (or large) attractive Casimir force for small (or large) d . In addition, the relative error becomes large for large d [see Fig. 5(b)], which indicates that the nonlocal effects become more and more important with increasing d . This is due to the fact that the difference of the effective permittivity for local and nonlocal cases is large in the low-frequency region, as shown in Fig. 1(a).

IV. CONCLUSION

In summary, we investigate the Casimir force between two infinite composite slabs containing nonlocal metallic nanoparticles. Based on nonlocal Mie scattering theory and beyond the electrostatic approximation, we develop an original theory for the equivalent local permittivity and permeability of a metallic nanosphere with spatially dispersive permittivity. Using a nonlocal Bruggeman effective medium theory and Maxwell-Garnett theory, we calculate the effective permittivity and permeability of the composite slabs, and then the nonlocal effect on the Casimir force between the inhomogeneous composite systems can be studied with Casimir-Lifshitz theory. We illustrate that the nonlocality on the Casimir force

is strongly dependent on the choice of effective medium theories, and the nonlocal effect becomes more significant for the composite media with symmetric microstructures than for those with asymmetric microstructures. Even for symmetric microstructures, the nonlocal effect becomes strongest at the percolation threshold.

Some comments are in order. The possibility of controlling the Casimir force using nonlinear materials with optical Kerr effects was pointed out [47]. Since the nonlinear materials are homogeneous, the applied field should be quite large to achieve available nonlinear responses and to control the transition between attractive force and repulsive force. In this connection, with the inhomogeneous composite materials, one can make use of the surface plasmon resonance to enhance the local fields in the nonlinear component and, hence, a small applied field may result in large nonlinearity and tunable Casimir force. More recently, the Casimir interaction torque in the composite system formed by a dense array of metallic nanowires embedded in dielectric fluids was studied, and the Casimir torque can be several orders of magnitude larger than the previous reports due to the ultrahigh density of photonic states in the nanowire array [48]. It is of interest to perform numerical calculations on the Casimir torque based on different effective medium models, emphasizing the spatial dispersion and percolation effect on the Casimir torque.

ACKNOWLEDGMENTS

This work was supported by the National Natural Science Foundation of China under Grants No. 11074183 and No. 11374223, the National Basic Research Program under Grant No. 2012CB921501, the Key Project in Natural Science Foundation of Jiangsu Education Committee of China under Grant No. 10KJA140044, the Ph.D. Programs Foundation of the Ministry of Education of China (Grant No. 20123201110010), the Natural Science Foundation of Jiangsu Education Committee of China (Grants No. 13KJB140015 and No. 13KJB140017), and the Project Funded by the Priority Academic Program Development of Jiangsu Higher Education Institutions.

-
- [1] H. B. G. Casimir, Proc. K. Ned. Akad. Wet. **51**, 793 (1948).
 - [2] M. Bordag, U. Mohideen, and V. M. Mostepanenko, *Phys. Rep.* **353**, 1 (2001).
 - [3] H. B. Chan, V. A. Aksyuk, R. N. Kleiman, D. J. Bishop, and F. Capasso, *Science* **291**, 1941 (2001).
 - [4] E. M. Lifshitz, Sov. Phys. JETP **2**, 73 (1956).
 - [5] M. S. Tomaš, *Phys. Rev. A* **66**, 052103 (2002).
 - [6] C. Raabe, L. Knöll, and D. G. Welsch, *Phys. Rev. A* **68**, 033810 (2003).
 - [7] F. S. S. Rosa, D. A. R. Dalvit, and P. W. Milonni, *Phys. Rev. Lett.* **100**, 183602 (2008).
 - [8] I. Pirozhenko, A. Lambrecht, and V. B. Svetovoy, *New J. Phys.* **8**, 238 (2006).
 - [9] A. Lambrecht, I. Pirozhenko, L. Duraffourg, and Ph. Andreucci, *Europhys. Lett.* **77**, 44006 (2007).
 - [10] V. B. Svetovoy, P. J. van Zwol, G. Palasantzas, and J. Th. M. De Hosson, *Phys. Rev. B* **77**, 035439 (2008).
 - [11] R. Zhao, J. Zhou, Th. Koschny, E. N. Economou, and C. M. Soukoulis, *Phys. Rev. Lett.* **103**, 103602 (2009).
 - [12] J. N. Munday, F. Capasso, and V. A. Parsegian, *Nature (London)* **457**, 170 (2009).
 - [13] R. Zeng, Y. P. Yang, and S. Y. Zhu, *Phys. Rev. A* **87**, 063823 (2013).
 - [14] R. Esquivel-Sirvent, *J. Appl. Phys.* **102**, 034307 (2007).
 - [15] M. G. Silveirinha and S. I. Maslovski, *Phys. Rev. A* **82**, 052508 (2010).
 - [16] A. Gusso and U. B. Reis, *Europhys. Lett.* **99**, 36003 (2012).
 - [17] F. S. S. Rosa, D. A. R. Dalvit, and P. W. Milonni, *Phys. Rev. A* **84**, 053813 (2011).

- [18] S. I. Goto, A. C. Hale, R. W. Tucker, and T. J. Walton, *Phys. Rev. A* **85**, 034103 (2012).
- [19] W. M. R. Simpson, S. A. R. Horsley, and U. Leonhardt, *Phys. Rev. A* **87**, 043806 (2013).
- [20] S. A. R. Horsley and W. M. R. Simpson, *Phys. Rev. A* **88**, 013833 (2013).
- [21] R. Esquivel-Sirvent and G. C. Schatz, *Phys. Rev. A* **83**, 042512 (2011).
- [22] J. Sun, X. K. Hua, A. V. Goncharenko, and L. Gao, *Phys. Rev. A* **87**, 042509 (2013).
- [23] E. I. Kats, *Sov. Phys. JETP* **46**, 109 (1977).
- [24] R. Esquivel, C. Villarreal, and W. L. Mochan, *Phys. Rev. A* **68**, 052103 (2003).
- [25] R. Esquivel and V. B. Svetovoy, *Phys. Rev. A* **69**, 062102 (2004).
- [26] R. Esquivel-Sirvent and V. B. Svetovoy, *Phys. Rev. B* **72**, 045443 (2005).
- [27] A. D. Hernández de la Luz and M. A. Rodríguez Moreno, *Braz. J. Phys.* **41**, 216 (2011).
- [28] R. Esquivel-Sirvent and G. C. Schatz, *J. Phys. Chem. C* **116**, 420 (2012).
- [29] R. Ruppin, *Phys. Rev. Lett.* **31**, 1434 (1973).
- [30] Y. Wu, J. S. Li, Z. Q. Zhang, and C. T. Chan, *Phys. Rev. B* **74**, 085111 (2006).
- [31] V. A. Yampol'skii, S. Savel'ev, Z. A. Mayselis, S. S. Apostolov, and F. Nori, *Phys. Rev. Lett.* **101**, 096803 (2008).
- [32] A. O. Sushkov, W. J. Kim, D. A. R. Dalvit, and S. K. Lamoreaux, *Nat. Phys.* **7**, 230 (2011).
- [33] Y. Huang and L. Gao, *J. Phys. Chem. C* **117**, 19203 (2013).
- [34] B. B. Dasgupta and R. Fuchs, *Phys. Rev. B* **24**, 554 (1981).
- [35] J. M. McMahon, S. K. Gray, and G. C. Schatz, *Phys. Rev. Lett.* **103**, 097403 (2009).
- [36] C. David and F. J. G. de Abajo, *J. Phys. Chem. C* **115**, 19470 (2011).
- [37] S. Raza, G. Toscano, A. P. Jauho, M. Wubs, and N. A. Mortensen, *Phys. Rev. B* **84**, 121412(R) (2011).
- [38] V. V. Datsyuk and O. M. Tovkach, *J. Opt. Soc. Am. B* **28**, 1224 (2011).
- [39] Y. X. Ni, L. Gao, and C. W. Qiu, *Plasmonics* **5**, 251 (2010).
- [40] A. K. Sarychev, R. C. McPhedran, and V. M. Shalaev, *Phys. Rev. B* **62**, 8531 (2000).
- [41] L. Gao, J. P. Huang, and K. W. Yu, *Phys. Rev. B* **69**, 075105 (2004).
- [42] L. Gao and K. W. Yu, *Phys. Rev. B* **72**, 075111 (2005).
- [43] D. Stroud and F. P. Pan, *Phys. Rev. B* **17**, 1602 (1978).
- [44] J. H. Huang and P. T. Leung, *J. Opt. Soc. Am. A* **30**, 1387 (2013).
- [45] Y. P. Yang, R. Zeng, H. Chen, S. Y. Zhu, and M. S. Zubairy, *Phys. Rev. A* **81**, 022114 (2010).
- [46] J. Sun and L. Gao, *Solid State Commun.* **152**, 1666 (2012).
- [47] C. H. Raymond Ooi and Y. Y. Khoo, *Phys. Rev. A* **86**, 062509 (2012).
- [48] T. A. Morgado, S. I. Maslovski, and M. G. Silveirinha, *Opt. Express* **21**, 14943 (2013).